Bibliographical reference

Transient SEA Studies on the Damping of Coupled Building Elements, C. Kling and W. Scholl, Acta Acustica **vol. 97** (Number 2), 2011, pp. 266-277

DOI
https://doi.org/10.3813/AAA.918406

Acta Acustica united with Acustica
Vol. 97 (2011) 266 – 277

DOI 10.3813/AAA.918406

Transient SEA Studies on the Damping of Coupled Building Elements

C. Kling, W. Scholl
Physikalisch-Technische Bundesanstalt (PTB), Bundesallee 100, D-38116 Braunschweig, Germany.
christoph.kling@ptb.de

Summary
The airborne sound insulation of building elements depends on the global mechanical damping of the construction. The structural reverberation time is used to derive that quantity. However, the reverberation process combines the responses of the interconnected systems and this could lead to misinterpretations. Transient Statistical Energy Analysis (TSEA) is applied to highlight this effect. The results are compared with measurements in scale models.

PACS no. 4340.-r, 43.50.Jh, 43.55.Rg, 43.58.-e

1. Introduction

Damping is an important characteristic in building acoustics. It considerably influences the sound reduction index of building elements. According to Cremer and Heckl [1] (c.f. also [2]), the sound reduction index of a homogeneous wall gains $10\lg(\eta)$ [dB] with its damping factor η. Doubling up the damping, thus, would result in an increase of the sound reduction by 3 dB on the one hand. Neglecting the same amount of damping of a tested wall in a laboratory would result in an uncertainty of about 3 dB on the other hand (which is a realistic value, considering the large range of boundary conditions allowed by the measurement standard [3]). Thus, there is a large interest in determining the damping of building elements, in particular when installed in an acoustic test facility or in a building.

The influence of adjacent building elements and air-filled volumes on the sound reduction index of a building element is expected to be completely represented by the influence on its damping factor. It is assumed that the resulting damping of a building element, called the *total damping factor* η_{total}, is given by the sum of the losses via sound radiation, sound transmission through the edges of the element and by internal or material damping [4],

$$\eta_{\text{total}} = \eta_{\text{internal}} + \eta_{\text{radiation}} + \eta_{\text{edgelosses}}. \tag{1}$$

This sum then should be directly observable at the respective building element. In practice it is mostly measured through the structural reverberation time T (in s) by

$$\eta = \frac{2.2}{fT}, \tag{2}$$

with centre frequency f (in Hz) of the observed third-octave or octave frequency band. When a few years ago the idea came up to use this simple kind of measurement to correct laboratory measurement results of the sound reduction index (SRI) for the particular damping conditions in that laboratory, it became immediately obvious that only the edge losses should be used for correction; the other parts being essentially characteristics of the test object and not of the test facility. So the question arose how to determine experimentally the edge losses of a building element when installed in a building or in particular in a test facility for sound reduction index measurements. Such investigations were carried out in [5]. The result was, however, not as expected. The building element tested is not only subject to the leakage of energy but to, in general, unsteady flows of energy in both directions between the test object, the structure of the adjacent laboratory building and the airborne sound fields on both sides of the test objects. Reverberation decay curves observed on whichever element of the whole vibration system will reveal the instantaneous net energy flow of this element and will not represent any single damping factors nor time-independent sums of them. Carrying on using equation (2) will lead to apparently time-dependant damping factors. Although they appear strange, those time-dependant "apparent damping factors" are used within this paper for three reasons:

1. Calculating damping factors from decay curves via reverberation times according to equation (2) means a kind of derivation of the decay curve with respect to time. Changes in the slope of the reverberation, thus, become better visible, as can be seen below.
2. The "apparent damping factors" may temporarily converge to real damping factors, when the power flow is directed only away from the considered building element and, thus, can be compared directly with damping factors known from physical considerations.

Received 5 July 2010,
accepted 17 January 2011.

3. But above all it seems necessary to deal with this widespread approach of neglected power reflow to demonstrate its limits and possibly erroneous conclusions

In the meantime, M. Schneider *et al.* have presented further investigations [6], based on [5]. They showed, that the influence of energy reflow decreases in extended buildings, compared with the situation of a laboratory for sound insulation measurements of walls. But as the laboratory situation is the basis for the rating of building elements and thus the basis for predictions of the performance of buildings, the following considerations are focussed on this worst case.

This paper concentrates on the interpretation of reverberation time measurements. Details of the mentioned scale model experiments and material investigations have already been published in [7] and [8].

2. SEA basics

To follow the reverberation analysis, a basic understanding of SEA principles and formulas is required, especially for the meaning of the apparent loss factor introduced here. So after the following crash course, the reader should be familiar with the concept of SEA in general and transient SEA (TSEA) in particular. For further reading, see for example [9], [10] or [11]. First works on the application of linearly coupled resonators on acoustical systems were performed in the early 1960s by Lyon [12, 13], Smith [14] and Maidanik [15]. Works especially issuing transient processes were written by Manning [16], Lyon [17] and Lai [18, 19]. Similar research on coupled spaces was performed in the field of room acoustics and is summarised in [20] or [21].

As the name implies, statistical energy analysis (SEA) deals with the statistical distribution of energy in a network of linearly coupled resonators [9]. If one of the resonators is excited, the coupling leads the introduced energy to be distributed among the network. The way energy flows through the network is determined by the coupling between the resonators. Moreover, each resonator is damped and, therefore, can dissipate part of its energy. Thus, if no more power is introduced to any of the resonators, the whole system reverberates until the noise level is reached.

For the application of this network model to reality, it is better to talk of subsystems instead of resonators. Each subsystem is an element or region in the total system that represents uniform properties and energy distribution. Usually when modelling a SEA system, the design goal is to get only a small number of subsystems.

Figure 1 shows the general model of a set of three subsystems with indices 1, 2 and 3, each containing energies E_1, E_2 and E_3. Due to the coupling, energy is distributed by the six power flows P_{ij} $(i, j = 1, 2, 3)$. Each subsystem can have an energy source feeding it with power P_{source1}, P_{source2} and P_{source3}. Finally due to damping, the subsystems dissipate powers P_{11}, P_{22} and P_{33}.

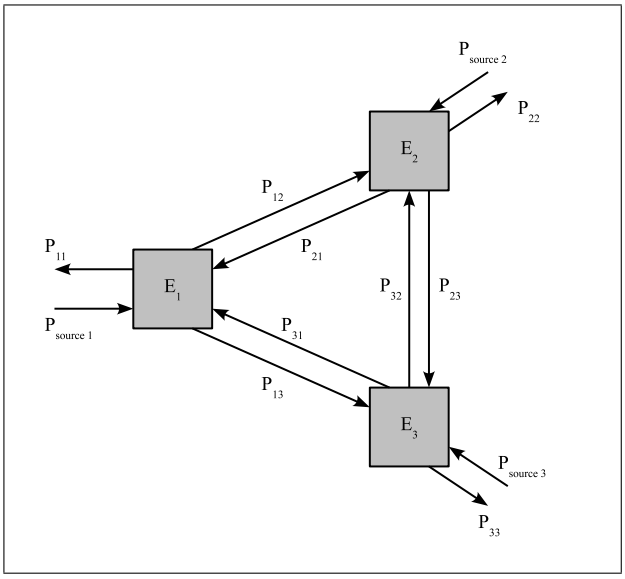

Figure 1. General model of SEA for three subsystems.

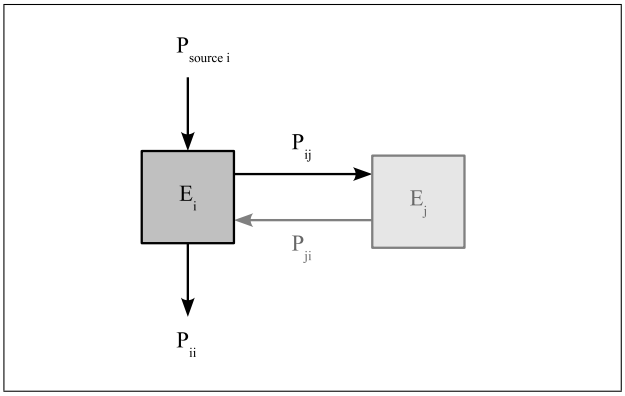

Figure 2. Sketch of a subsystem i with neighbour j showing all energy and power quantities directly related to i in the steady state.

2.1. Steady state

Usually, SEA is applied to the steady state, which means that any input power is held constant over time. This finally leads to an equilibrium of ingoing and outgoing powers in each subsystem, which means the energy E_i in each of the 6N subsystems i is constant,

$$\frac{\mathrm{d}}{\mathrm{d}t} E_i = 0 \quad \Leftrightarrow \quad E_i = \text{const.} \quad (i = 1, \ldots, N), \tag{3}$$

and all power flows P are constant, too. Figure 2 shows the steady state from the point of view of a certain subsystem i. Using the figure's notation, the power balancing equation of this subsystem can be written as

$$\begin{aligned} P_{\text{total in}} &= P_{\text{total out}} \qquad (i = 1, \ldots, N), \\ P_{\text{source}i} + \sum_{j(j\neq i)} P_{ji} &= P_{ii} + \sum_{j(j\neq i)} P_{ij}. \end{aligned} \tag{4}$$

The indices i and j both reach over the number of subsystems from 1 to N. Due to the linearity of coupling, the coupling power P_{ij} is proportional to the energy E_i of the

subsystem i from which the power originates. Moreover, the power increases with the number of cycles given by the resonance frequency ω, which is common to all subsystems and is an abstract and representative frequency for the group of modes in each subsystem. The remaining coefficient of proportionality η_{ij} is a constant number between zero and one, describing the fraction of the subsystem's i energy which is transmitted to subsystem j during one resonance cycle. The coefficient η_{ij} is called the *coupling loss factor*. This leads to the coupling power term

$$P_{ij} = \omega \eta_{ij} E_i. \tag{5}$$

Equivalently, the dissipation in each subsystem is assumed to depend on the subsystem energy E_i and the resonance frequency ω. The remaining coefficient of proportionality η_{ij} describes the fraction of the subsystem's i energy which is dissipated during one cycle. It is called the *dissipation loss factor*. The dissipation power term is written as

$$P_{ii} = \omega \eta_{ii} E_i. \tag{6}$$

Finally, the approach of the power-energy relation in equations (5) and (6) $P(t) = \omega\eta E(t) = -\mathrm{d}/\mathrm{d}t\, E(t)$ is equivalent to an exponential decay $E(t) = E_0 \exp(-\omega\eta t)$ (with starting energy E_0) of an excited system damped by the factor $\delta = \omega\eta$. For readability reasons, we summarise all loss factors of a certain subsystem i that represent a power loss and call this the *total loss factor* η_i of subsystem i,

$$\eta_i = \eta_{ii} + \sum_{j(j\neq i)} \eta_{ij}. \tag{7}$$

Using the terms for the coupling, dissipation and total loss factor, the power balancing equations for all subsystems can be rewritten and combined in a linear system of equations,

$$\begin{pmatrix} \eta_1 & -\eta_{21} & -\eta_{31} & \cdots & -\eta_{N1} \\ -\eta_{12} & \eta_2 & -\eta_{32} & \cdots & -\eta_{N2} \\ -\eta_{13} & -\eta_{23} & \eta_3 & \cdots & -\eta_{N3} \\ \vdots & \vdots & \vdots & \ddots & \vdots \\ -\eta_{1N} & -\eta_{2N} & -\eta_{3N} & \cdots & \eta_N \end{pmatrix} \cdot \omega \begin{pmatrix} E_1 \\ E_2 \\ E_3 \\ \vdots \\ E_N \end{pmatrix} = \begin{pmatrix} P_{\mathrm{source}1} \\ P_{\mathrm{source}2} \\ P_{\mathrm{source}3} \\ \vdots \\ P_{\mathrm{source}N} \end{pmatrix}. \tag{8}$$

$$\underline{\underline{\eta}} \cdot \omega \underline{E} = \underline{P_{\mathrm{source}}}.$$

This is the complete SEA model to be solved: The matrix $\underline{\underline{\eta}}$ of the loss factors η_{ij} gives a full description of the physical properties of all subsystems and their joints. The vector $\underline{P_{\mathrm{source}}}$ presents the input power flows into the particular subsystems. The solution vector $\underline{E}$ contains the subsystem energies which arise in the steady state of constant power inputs.

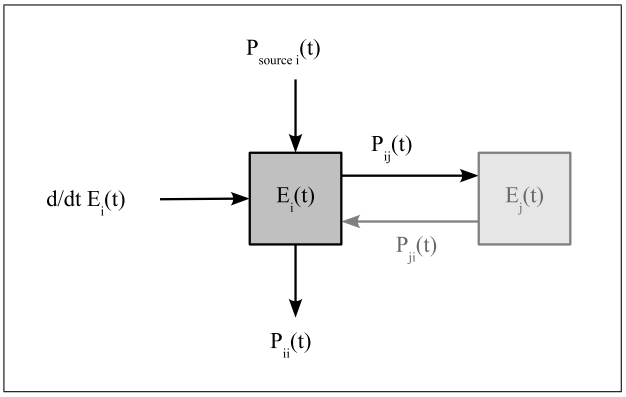

Figure 3. Sketch of a subsystem i with neighbour j showing all energy and power quantities directly related to i in the transient state.

2.2. Transient state

For studying a transient state, we must allow a subsystem's energies and power flows to vary in time,

$$\frac{\mathrm{d}}{\mathrm{d}t} E_i(t) \neq 0 \quad \Leftrightarrow \quad E_i(t) = \text{const.} \tag{9}$$

Figure 3 shows the transient state from the point of view of a certain subsystem i. Equivalently to the steady state case, we find the general power balancing equation of TSEA with the figure's notation as

$$\begin{aligned} \frac{\mathrm{d}}{\mathrm{d}t} E_i(t) &= P_{\text{total in}}(t) - P_{\text{total out}}(t), \\ &= P_{\text{source}i}(t) + \sum_{j(j\neq i)} P_{ji}(t) \\ &\quad - P_{ii}(t) - \sum_{j(j\neq i)} P_{ij}(t). \end{aligned} \tag{10}$$

Here, summands with a negative sign mean a loss for subsystem i, summands with a positive sign mean a gain for subsystem i. Using the time-variant power terms

$$\begin{aligned} P_{ii}(t) &= \omega \eta_{ii} E_i(t) \quad \text{Dissipation loss} \\ P_{ij}(t) &= \omega \eta_{ij} E_i(t) \quad \text{Coupling loss to subsystem } j \\ P_{ji}(t) &= \omega \eta_{ji} E_j(t) \quad \text{Coupling gain from subsystem } j \end{aligned} \tag{11}$$

the change in a subsystem's energy is written as

$$\frac{\mathrm{d}}{\mathrm{d}t} E_i(t) = P_{\text{source}i}(t) + \sum_{j(j\neq i)} \omega \eta_{ji} E_j(t) - \omega \eta_i E_i(t). \tag{12}$$

Please note that the time-variance only applies to the power and energy quantities but not to the loss factors. All loss factors, both dissipation and coupling, are time-invariant. These completely define the physical behaviour and, thus, the system remains a linear time-invariant (LTI) system.

2.3. Reverberation process

For the special case of a reverberant decay, we assume that some energy was introduced to the system sometime in the

past ($t < 0$) and from now on ($t \geq 0$), the system continues to distribute and dissipate this energy in the network. In reverberation measurement, we are interested in the loss of energy of a subsystem, namely in the effective power loss $P_{\mathrm{loss}i}(t)$. Without any power sources, this is expressed as

$$P_{\mathrm{loss}i}(t) := -\frac{\mathrm{d}}{\mathrm{d}t} E_i(t) = \omega \eta_i E_i(t) - \sum_{j(j\neq i)} \omega \eta_{ji} E_j(t). \quad (13)$$

2.4. Numerical implementation

For numerical implementation, the timeline is discretised into (small enough) finite intervals Δt, leading to a time series t_n ($n = 0, 1, 2, \ldots$). The energy variation in subsystem i in the decaying system then turns to

$$-\frac{\mathrm{d}}{\mathrm{d}t} E_i(t) \rightarrow \frac{E_i(t_{n+1}) - E_i(t_n)}{\Delta t}. \quad (14)$$

The subsystem energies can be calculated recursively from any time t_n for the next time sample t_{n+1} if a set of starting energies $E_0(t_0)$ at starting time t_0 is given,

$$E_i(t_{n+1}) = E_i(t_n) - \Delta t \, P_{\mathrm{loss}i}(t_n), \quad (15)$$

where $P_{\mathrm{loss}i}(t_n)$ is calculated as defined in equation (13) for $t = t_n$.

3. SEA analysis of damping measurement procedure

As mentioned before, relation (2) is generally used to determine the damping of a building element. First, the element of interest is excited with a signal and then, the reverberation time T is determined from the energy decay curve. This finally leads to the damping loss factor η.

In the following, the reverberation process is analysed by the use of the transient SEA concept. We start with the time-dependent power balance and, assuming exponential decay, derive an expression for the loss factor that apparently damps the element (subsystem) under test. This is performed for two models: First, the simple model of the present view is treated which leads to the known relations. Secondly, the simple model is expanded by power reflow from the adjacent elements and treated the same way as before. This consequently leads to a more complex expression of the apparent loss factor.

3.1. Simple model of the present view

Typical elements for reverberation measurement in building acoustics are rooms and walls. Since SEA only relates to energies, it does not matter if there are airborne sound fields or structure-borne sound fields. In the simple model, as used currently in practice (c.f. annex C in [4] or annex E in [22]), it is assumed that an excited element just looses its energy by dissipation and by coupling to adjacent elements (again walls and rooms). Any feedback of energy is neglected. Therefore, the only power flow is directed outwards by the primarily excited element. Figure 4 gives a sketch of a corresponding SEA model restricted to three subsystems for clarity. Even though the type of subsystem in SEA does not matter, the reader may think of an excited wall (subsystem 1) with an adjacent room (subsystem 2) and an adjacent wall (subsystem 3) as its direct neighbours.

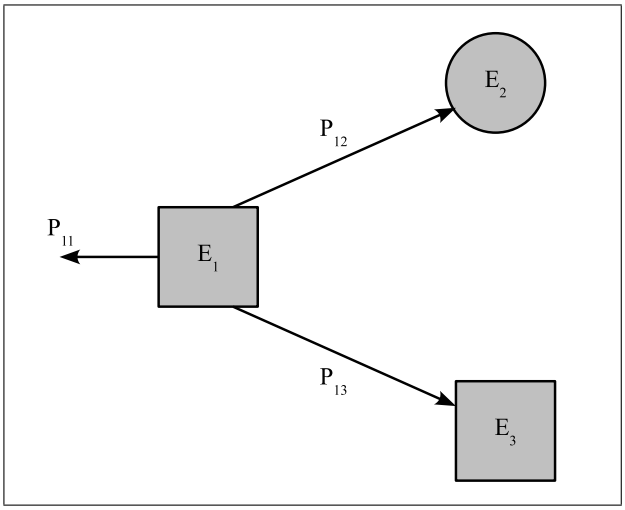

Figure 4. Sketch of an excited subsystem 1 (e.g. partition wall) with two neighbours 2 (e.g. adjacent room) and 3 (e.g. flanking wall) neglecting any power reflow.

Neglecting any reflow, the power balance of the excited subsystem 1 becomes

$$\begin{aligned} P_{\mathrm{loss}1}(t) &= -\frac{\mathrm{d}}{\mathrm{d}t} E_1(t) \quad (16)\\ &= P_{11}(t) \quad \text{(dissipation loss)}\\ &\quad + P_{12}(t) + P_{13}(t) \quad \text{(coupling losses)}. \end{aligned}$$

The sign of the energy change is negative because all power terms are losses here. Using the relations (11) for dissipation power loss and coupling power loss, we find

$$P_{\mathrm{loss}1}(t) = \omega\left(\eta_{11} + \eta_{12} + \eta_{13}\right) E_1(t). \quad (17)$$

Assuming exponential decay in the excited element, this means the whole system of three subsystems reverberates with the combined loss factor which is just the total loss factor of the excited subsystem 1,

$$P_{\mathrm{loss}1}(t) = \omega \eta_{\mathrm{total}1} E_1(t), \quad (18)$$

where $\eta_{\mathrm{total}1}$ is just the sum of the outgoing loss factors (dissipation and coupling). Of course, it is a constant value because its summands are time-invariant system quantities.

Hence, following this simple model, the loss factor determined by a standard reverberation measurement at element i is just the total loss factor of that element,

$$\eta_{\mathrm{total}1} = \eta_{ii} + \sum_{j(j\neq i)} \eta_{ij}. \quad (19)$$

Please note that there is no time dependency left in the loss factor. Therefore, the regarded subsystem would decay with its total loss factor exponentially until the noise level is reached.

Relation (19), which we derived here by using the SEA concept, is the generalised form of equation (1). According to this model, each building element is damped uniformly by its own characteristic total loss factor. Following this, the reverberation process can be used with relation (2) to determine the (total) damping.

3.2. Expanded model including power reflow

In contrast to the simplified view, we examine here the complete SEA model which not only includes power loss but also power reflow from the neighbouring subsystems. This expanded model is the completion of the simple model and includes the feedback-free case. A sketch of this model is shown in Figure 5, again restricted to three elements for clarity.

The power balance is now written as

$$\begin{aligned} P_{\text{loss}1}(t) \;=\; & P_{11}(t) && \text{(dissipation loss)} \\ & + P_{12}(t) + P_{13}(t) && \text{(coupling losses)} \\ & - P_{21}(t) - P_{31}(t) && \text{(coupling gains),} \end{aligned} \tag{20}$$

and using relations (11) for the power losses and power gains, we find

$$\begin{aligned} P_{\text{loss}1}(t) \;=\; & \omega\big(\eta_{11} + \eta_{12} + \eta_{13}\big) E_1(t) \\ & - \omega\eta_{21} E_2(t) - \omega\eta_{31} E_3(t). \end{aligned} \tag{21}$$

Comparing this to the equivalent equation (17) of the simple model, the system power loss is somewhat smaller, because the neighbours feed back some energy to subsystem 1.

How would an equivalent loss factor of the total system then look?

Since this is the loss factor that we would apparently observe when using the simple model, we call it the *apparent loss factor*. We can use the definition just as above,

$$P_{\text{loss}1}(t) \;=\; \omega\eta_{\text{apparent}1}(t) E_1(t). \tag{22}$$

So what we have in mind is a general loss factor corresponding to the known exponential decay of the system. If we use this definition in equation (20), we can solve the equation for $\eta_{\text{apparent}1}$ as

$$\begin{aligned} \eta_{\text{apparent}1}(t) \;=\; & \eta_{11} + \eta_{12} + \eta_{13} \\ & - \eta_{21}\frac{E_2(t)}{E_1(t)} - \eta_{31}\frac{E_3(t)}{E_1(t)}. \end{aligned} \tag{23}$$

This equation shows the detailed composition of the apparent loss factor which the element under test decays with. The relation (23) contains two main issues:

1. The loss factor we apparently observe in a measurement is smaller than the total loss factor.
2. This apparent loss factor is time-dependent because of the time-dependency of the subsystem energies. Both issues of the feedback model are contradictory to the previously discussed simple model.

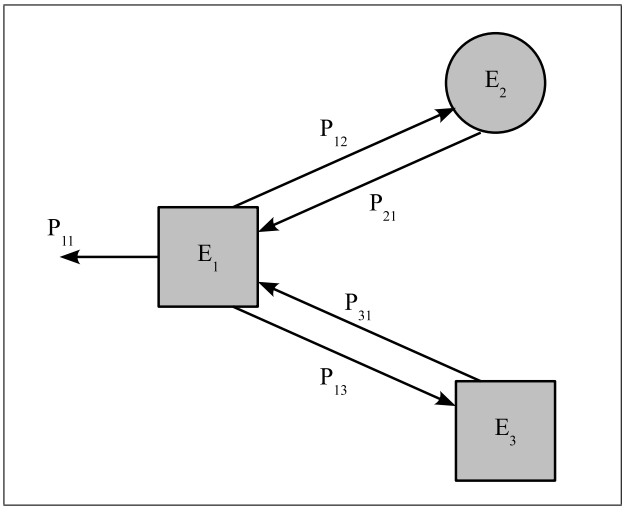

Figure 5. Sketch of an excited subsystem 1 (e.g. partition wall) with two neighbours 2 (e.g. adjacent room) and 3 (e.g. flanking wall) including the power reflow.

In the general case, for a subsystem i under test with neighbours j this equation is expressed as

$$\begin{aligned} \eta_{\text{apparent}i}(t) \;=\; & \eta_{ii} + \sum_{j(j\neq i)} \eta_{ij} && \text{(total loss factor)} \\ & - \sum_{j(j\neq i)} \eta_{ji}\frac{E_j(t)}{E_i(t)} && \text{(feedback terms).} \end{aligned} \tag{24}$$

This expression describes a loss factor that is found if the reverberation curve is analysed in the same way as with the simple model, but using several infinitely small time intervals instead of one large regression interval. We shall see that the apparent loss factor is an excellent tool for analysing the time-dependent influence of neighbours on an element under test. The TSEA simulations and direct measurements in the following show that this influence can not usually be neglected and that the use of the simple model then leads to bad results.

4. A wall test facility under test

The object being of particular interest here is a typical building acoustics wall test facility according to ISO 140 [3]. But instead of a full-scaled test facility, a small downscaled model was used for studying the energies and power flows. There are several advantages of such a model: The materials used are well-known and selected carefully. The facility design is restricted to the main elements and implements proper standard situations. Preliminary tests, especially on the joints, ensure reliable constructions. By contrast in a full-scaled wall test facility, the building construction, the execution of construction, the construction materials and the material properties are usually only roughly known. That is why, no reliable values can be determined for the dissipation and coupling loss factors which constitute the physical SEA model.

The downscaled facility, shown in Figure 6, implements a fully functional wall test facility on a scale of 1:10. Two

rooms (sending and receiving room) are separated by a partition wall. All dimensions meet the requirements of the standard [3] for wall test facilities on the reduced scale. The building acoustics frequency range of 100 Hz to 5 kHz is up-scaled to the model frequency range of 1 kHz to 50 kHz. The construction materials are selected in such a manner that material properties of typical building materials such as sand-lime bricks are mapped to the up-scaled frequencies. All mechanical material properties such as Young's modulus, shear modulus and material damping were determined from experiments for all frequencies required [8].

The model construction consisted of monolithic plates which were either rigidly connected by gluing over the entire face surfaces, or flexibly connected by using an elastic silicone layer. The junctions proved to be close to the ideal computable case. The suitability of the downscaled model as a wall test facility was validated extensively in [7]. In that reference, the reader will also find constructional details of the downscaled models and sound insulation indices compared to a typical wall test facility.

Two different partition walls were mounted rigidly into the model: A 'thin' wall of 3 mm acrylic glass (coincidence at about 10 kHz) corresponding to a lightweight 3 cm gypsum plasterboard wall (coincidence at about 1 kHz), and a 'thick' wall of 25 mm acrylic glass (coincidence at about 1.25 kHz) corresponding to a heavy 24 cm sand-lime brick wall (coincidence at about 125 Hz). The flanking walls were made of 25 mm acrylic glass plates.

4.1. SEA simulation model

To apply the SEA model in practise, first the system under test must be divided into subsystems. In building acoustics, the physical elements are walls, floors, ceilings and rooms, all containing structure-borne or airborne sound fields. For these elements, the coupling conditions of SEA are sufficiently satisfied. The subsystem energies of SEA are proportional to the time- and space-averaged squared field quantities of the building elements: The energy of a wall relates to the structure-borne sound velocity (usually, bending motion is sufficient) and the energy of a room relates to the airborne sound pressure. The power input into a room is achieved by a loudspeaker and the input into a wall by a shaker.

The loss factors, which define the physical model, result from material properties, geometry and joint design: The internal loss factor of the acrylic glass walls were set to the measured material damping coefficient of the complex bending stiffness, see [8]. The internal loss factors of the rooms were derived from reverberation time measurements. The coupling loss factors were implemented as follows: The wall-wall coupling was calculated according to Craik [Diss29], the wall-room coupling was calculated with the radiation efficiency according to Leppington [Diss43], the room-wall coupling arose from the reciprocal wall-room coupling, and the non-resonant direct room-room coupling was computed according to Sewell [Diss42]. More details can be found in [5].

Figure 6. Miniature model of a wall test facility on a scale of 1:10. The outer dimensions are about 1 m × 0.45 m × 0.35 m. The flanking walls are made of 25 mm acrylic glass plates; a plate of 3 mm acrylic glass is used as a thin partition wall here.

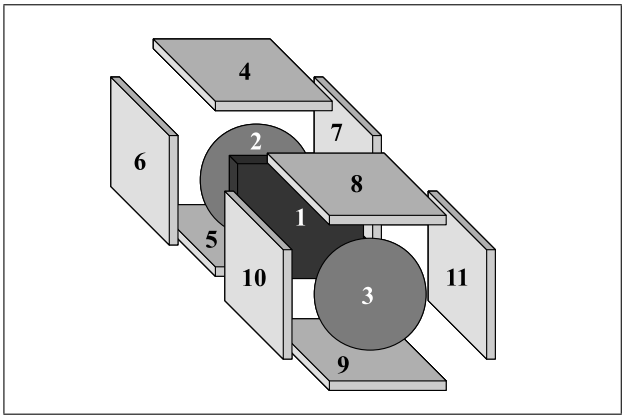

Figure 7. Sketch of the implemented SEA model for a wall test facility. The individual subsystems are: (1) partition wall, (2) sending room, (3) receiving room, (4–7) ceiling, floor and walls on the sending side, (8–11) ceiling, floor and walls on the receiving side.

Figure 7 shows the SEA model implemented here. Eleven subsystems were used: the partition wall, the eight flanking walls on either side including the floors and the ceilings and the two air volumes of the sending and receiving rooms. In the following, the partition wall is of special interest. That is why, it is sufficient to include only its nearest neighbours and the partition itself in the model. Remote subsystems, such as the rear walls and the air volume outside of the test facility, contain only sparse energy. Thus, they hardly affect the network and can be neglected in SEA.

The idealised construction and well-known material properties of the miniature model allow us to apply different generally acknowledged assumptions about plate motion, material damping and coupling at joints. From this mixture of experimental data and physical models, the loss factor matrix (as shown in equation (8)) of the downscaled test facility could be set up. Details and validation of the loss factor matrix determination can be found in [5]. This is the basis of the following transient computations. Applying this method to a real wall test facility, including all its roughly known materials and construction details, would probably result in non-reliable simulations. A more measurement-based method would have to be used in that case.

4.2. Experimental setup

In addition to the TSEA simulation, reverberation measurements were performed in the downscaled wall test facility for the simulated setups. As in the TSEA simulation, impulse excitation was used in experiment: Impulses to walls were directly injected by an impact hammer, impulses to rooms were indirectly injected by means of sweep excitation followed by an impulse response calculation.

For each excitation, the field quantities of the sound fields were measured in different subsystems simultaneously, each at several locations for spatial averaging: Accelerometers were used for the measurement of sound velocity on walls and microphones were used for sound pressure measurements. Since time plots of subsystem energies are the direct output of TSEA, for comparison, velocity and pressure signals were used to calculate the wall and room energies, respectively,

$$E_{\mathrm{room}}(t) = \frac{V_{\mathrm{room}}}{\rho_{\mathrm{air}} c_{\mathrm{air}}^2} \overline{p^2(t)}, \tag{25}$$

$$E_{\mathrm{wall}}(t) = 2E_{\mathrm{kin}}(t) = m\overline{v^2(t)}, \tag{26}$$

where V_{room} is the room's volume, ρ_{air} ($\approx 1.29\,\mathrm{kg/m^3}$) is the density of air and c_{air} is the speed of sound in air, and m is the mass of the wall. The formulas (25) and (26) derive from the mechanical energies of the subsystems, being the sum of potential and kinetic energies. $\overline{p^2(t)}$ and $\overline{v^2(t)}$ are the time- and space-averaged squared values of the measured velocity and pressure signals, respectively.

The measurements allow direct comparison of real and simulated time behaviour and, thus, give an additional validation for the SEA model and the TSEA computations.

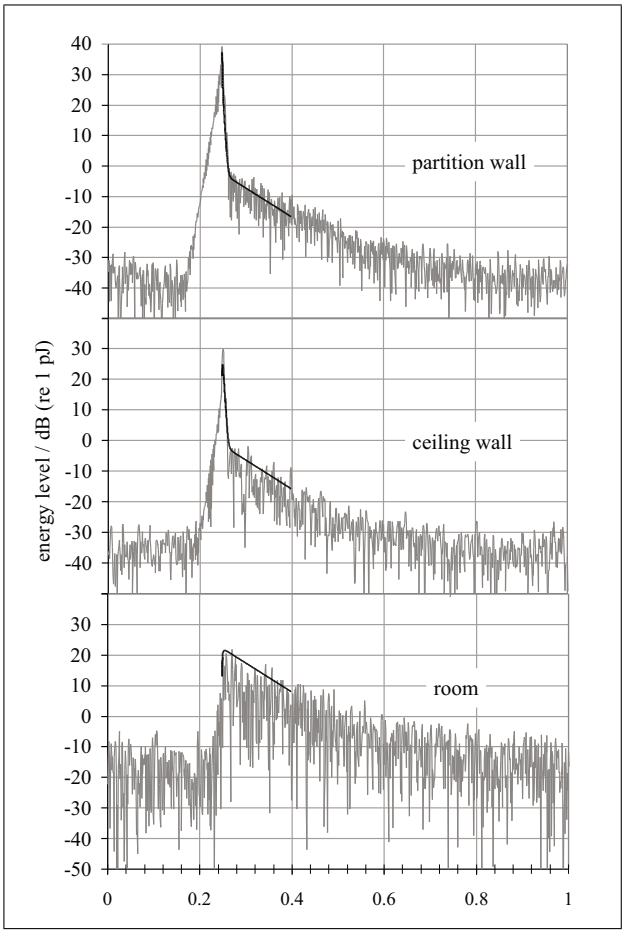

Figure 8. Energy levels as measured and as simulated including power reflow from adjacent elements during impulse excitation of the partition wall: (top) on partition, (mid) on ceiling, (bottom) in room.

4.3. Results of simulation and measurement

We have not presented all validation measurements here, because we want to highlight the transient behaviour of a coupled system. Instead, we are showing an example of the situation with impulse excitation of the thick wall in the 2 kHz third-octave band. Moreover, we have restricted the plots to three subsystems as an example: the excited partition wall, a flanking wall and an adjacent room. The other subsystems behave equivalently.

Figure 8 shows the measured and simulated energy levels of the three subsystems in a time plot. Due to the small dimensions, the observable part of the decay process ends within a second. For comparison to a full scaled wall test facility, the values on the time axis have to be multiplied by the model scale, i.e. 10 in this case. The experimental curves contain the background noise of the sensors especially observable at the initial 200 ms time interval and at the final 200 ms time interval of the plots. The TSEA simulated curves are the black dashed lines on the top. Since the simulation yields statistically averaged energy values, its curves are flat.

The relatively slow ramp just before the impulse maximum in the experimental curves is a filter effect. Due to the short decay times, time-inverse filtering is required. This results in rapidly increasing signals to be covered by the filter response but allows quickly decreasing signals (in which we are interested in) to be unaffected.

The measured curve of the excited wall (Figure 8a) firstly shows a fast decay rate of about 40 dB/s of energy decrease and then a slow decay until the noise level is reached. The energy curve of the flanking wall (Figure 8b) behaves the same way except for a smaller peak at the beginning. The energy curve of the adjacent room (Figure 8c) lacks the strong peak but also shows the slow decay.

Now the question arises as to which of the above theories can explain the experimental time behaviour of the three elements? The simple model is mainly restricted to the excited subsystem, namely the partition wall. Following equation (18), the energy of the partition wall would exponentially decrease with the total loss factor of the wall. According to equation (19), this total loss factor consists of several constant parts and is, therefore, time-independent and characteristic for the element. A log(energy)-over-time-plot would, therefore, present a straight decreasing slope. The experimental curves behave

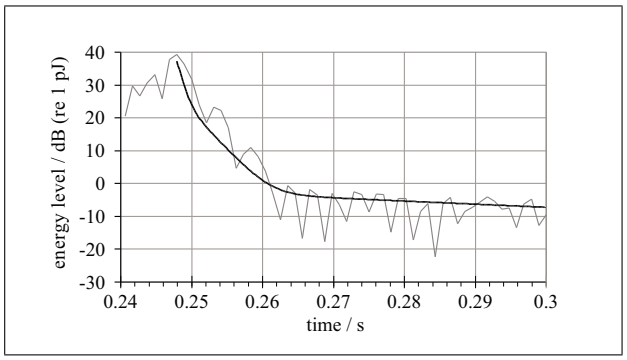

Figure 9. Detailed view of the fast decay of the partition wall as measured and simulated after impulse excitation.

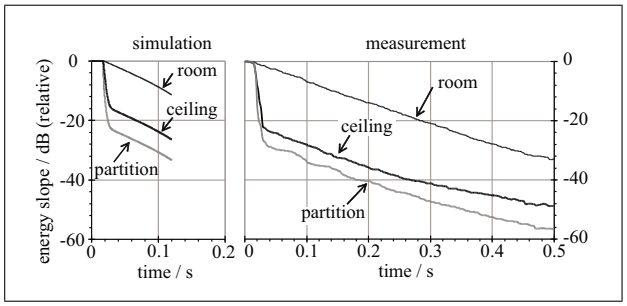

Figure 10. Energy slope of the partition wall, a flanking wall and an adjacent room (left) as simulated including the power reflow and (right) as determined from experimental data.

contrary to this prediction. Indeed, a close up of the first strong slope of the partition wall curve in Figure 9 highlights that even the strong decay at the beginning apparently consists of several time regions with different decay rates.

As the diagrams show, the feedback model meets the experimental energy-time-curves far better. A better comparison can be achieved by time-plots of backward-integrated energies. Moreover, that kind of plot is used for reverberation time evaluation. This is presented for the above example in Figure 10. The agreement between the experimental and the TSEA-simulated curves is good. As a first result, we find a uniform decay rate in all elements for later times. As we will see, the reverberation time in this region is just the reverberation time of the adjacent room. This means, the whole system, including the excited partition, decays uniformly with the rate of the room. This is definitely not in agreement with the simple model.

The analysis on the basis of energy-time plots, such as in Figures 8, 9 and 10, provides only limited insights. As a big advantage, the TSEA enables us to perform extended analysis and to have a detailed insight into the system's time behaviour. Since energies and power flows are the fundamental quantities in TSEA, the completed simulation yields the energy of any subsystem and the power flow between any two elements for all simulated time points. In fact, the simulation of the wall test facility provides a large amount of data that has to be arranged concisely. This is performed in the following for three standard situations of building acoustics.

5. Detailed analysis of simulated reverberation

In building acoustics, there are two typical kinds of reverberation processes: structure-borne sound reverberation of a partition wall and airborne sound reverberation of a (receiving) room. Both situations were simulated by TSEA, including the feedback effect, and analysed in more detail. For the structure-borne case, a thick partition as well as a thin partition wall were investigated as described before. Both partition walls were rigidly connected to the flanking facility walls. All flanking walls were thick walls. Thus, three different reverberation situations have been analysed:

- impulse excitation of a thick partition wall,
- impulse excitation of a thin partition wall,
- impulse excitation of a room.

The simulation results are presented for each situation by means of four diagrams (Figures 11, 12 and 13). The first diagram is a time-plot of the subsystem energy levels (upper left curve). The second is a time-plot of the power levels (upper right curve). To highlight the direction of power flow, the two power flows through the joint between two subsystems are combined to an effective power loss $P_{\text{effectiveloss1}}$. Hence, a positive value shows a flow from subsystem 1 to subsystem 2 (a loss to 1), a negative value shows a flow in the reverse direction from subsystem 2 to subsystem 1 (a gain to 1).

$$\begin{aligned} P_{\text{effectiveloss1}}(t) &= \text{loss} - \text{gain} = P_{12} - P_{21} \\ &= \omega\eta_{12}(t)E_1(t) - \omega\eta_{21}(t)E_2(t). \end{aligned} \tag{27}$$

Because power levels are used, values below the reference value of 10^{-12} W, meaning levels below 0 dB (ref 10^{-12} W), are not shown in the upper right curve of the following diagrams. This kind of plot might be unusual but it clearly demonstrates the directivity of power flows and, thus, makes clear which subsystem is the effective sender and which is the effective receiver of energy.

The last two diagrams use the apparent loss factor as introduced before. The time plot of this virtual quantity (lower left curve) shows the effective value that damps the partition wall. The separation of the individual feedback terms of the apparent loss factor gives the influence of each neighbouring subsystem (lower right curve).

Although eleven subsystems were included in the simulation, the following plots only show three subsystems for better clarity: The partition, the ceiling on the receiving side and the receiving room. The other seven flanking walls and the sending room behave similarly to the receiving ceiling and the receiving room, respectively. Again, we restrict ourselves to the 2 kHz third octave band for demonstration. Other frequency bands show similar behaviour.

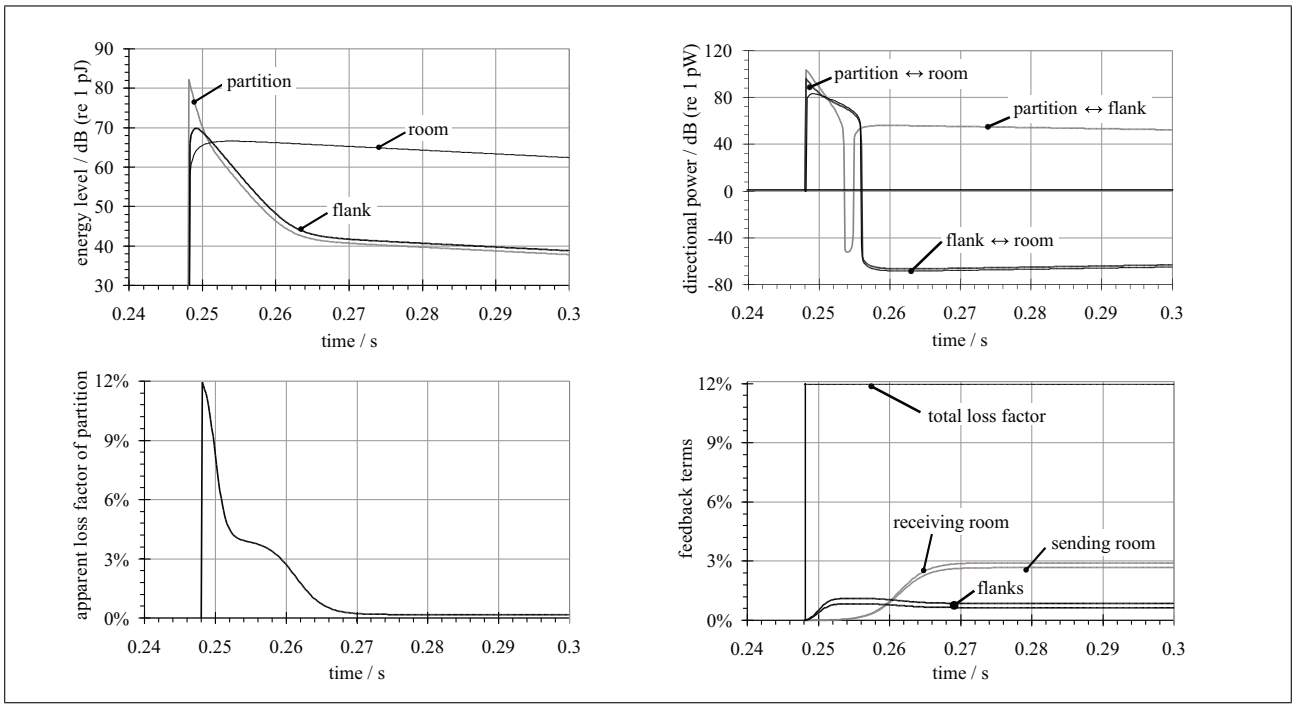

Figure 11. Time plots of (top left) energy level, (top right) power flow, (bottom left) apparent loss factor and (bottom right) feedback terms for the case of impulse excitation of the thick partition wall.

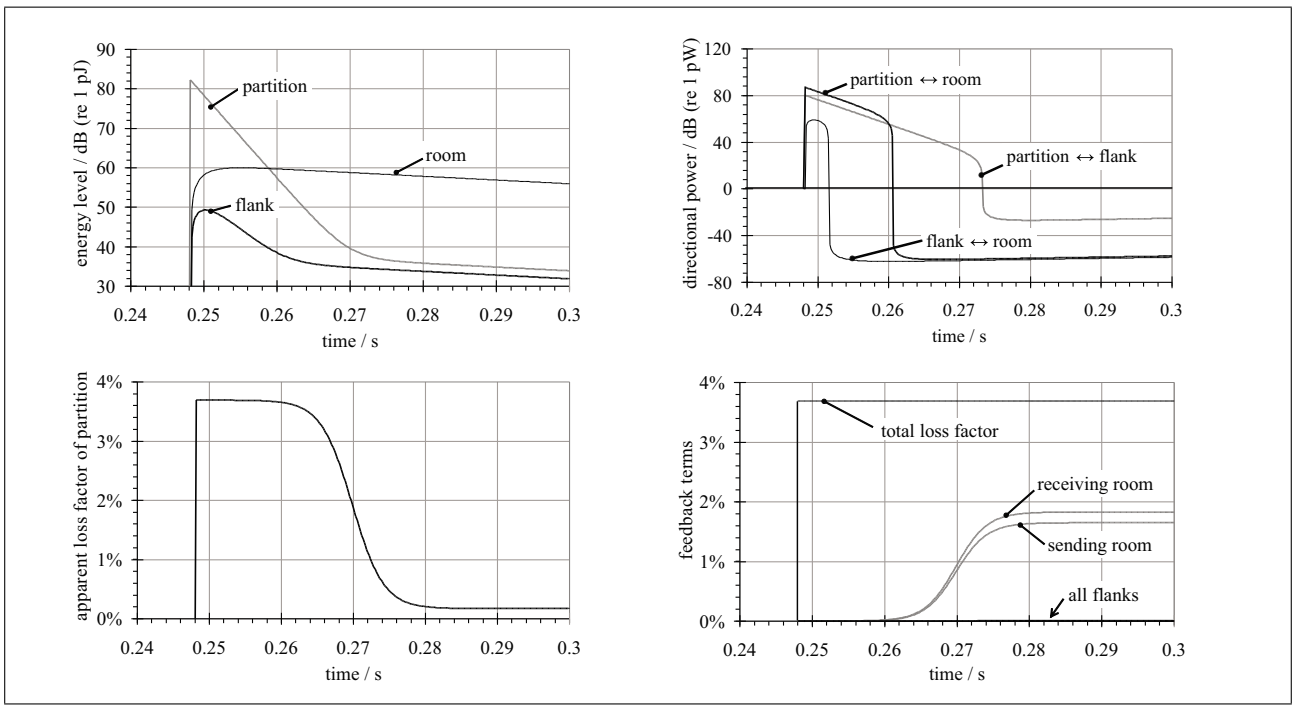

Figure 12. Time plots of (top left) energy level, (top right) power flow, (bottom left) apparent loss factor and (bottom right) feedback terms for the case of impulse excitation of the thin partition wall.

5.1. Impulse excitation of a thick partition wall

Relates to Figure 11. The simulation starts some time before the impact which is introduced to the partition wall approximately at 248 ms. This time point is arbitrary. For this theoretical point of time, all the energy is located in the partition (see upper left plot). Immediately after the impact, the energy is distributed to the neighbouring subsystems: A flanking wall and a room. Thus, the energy of the partition decreases whereas the energies of the neighbouring subsystems increase. Since the flanking walls are of the same type of element as the partition, the coupling is good and the flanking walls soon reach a similar energy level to the partition itself. Looking at the corresponding

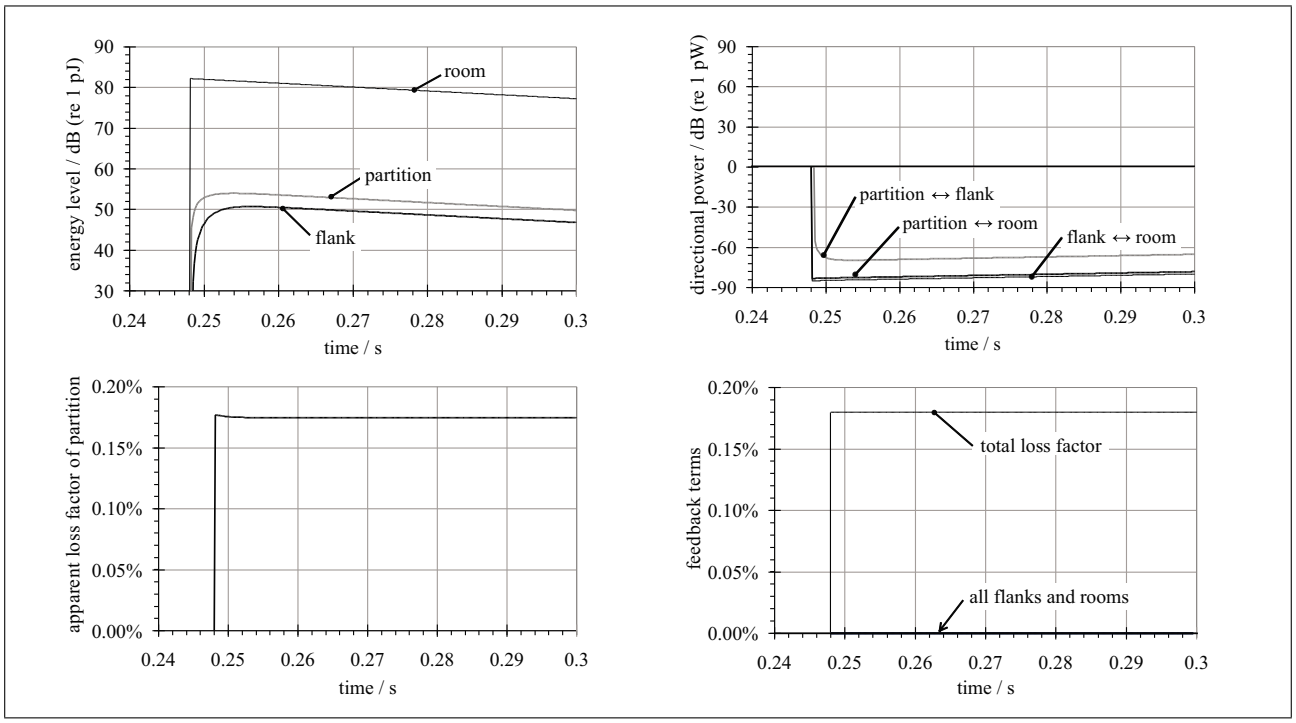

Figure 13. Time plots of (top left) energy level, (top right) power flow, (bottom left) apparent loss factor and (bottom right) feedback terms for the case of impulse excitation of the room.

power flows in the upper right plot, we find that the power flow from the partition to the neighbours is not constant but decreases immediately after the impact. Moreover, the power flow from the partition to the ceiling changes its direction between approximated time points 253 ms and 255 ms. At time point 256 ms, the exchange of energy between the walls and the room changes direction and the walls are now fed by the room. From the time point 265 ms on, the system reaches a kind of steady behaviour, meaning that the room works as an energy buffer feeding the walls and the walls dissipate the energy. A plot of energy level differences (which is not shown here) shows constant level differences between all subsystems. This state is held until a noise level is reached.

The lower left plot of the apparent loss factor shows the value of the total loss factor in the very first moment after the impact, immediately decreasing over time to a very small value of about 0.2% after the time point 270 ms. Between the time points 252 ms and 258 ms, a kind of a plateau is reached in the system. The reason for that can be seen in the lower right plot, where the separated feedback terms of the apparent loss factor demonstrate at which time which neighbour subsystem affect the reverberation process of the excited partition. The flanking walls have an immediate influence on the process and their feedback reaches a maximum at time point 252 ms. The rooms require more time to affect the reverberation effectively and their feedback starts at about 258 ms. Within this time interval there is only a feedback from the flanking walls, whereas the rooms charge with energy. After the time point of about 270 ms, the sum of the 10 feedback terms (8 flanking walls, 2 rooms) reduces the apparent loss factor to a very small value that is about the dissipation loss factor of a room. From now on, the rooms discharge their energy to the walls which immediately dissipate it.

An analysis of the simulated loss factor of the partition wall according to the standard [22] (uses T15 decay time with the energy slope) leads to a value of about 4%. This T15 analysis can be reconstructed in Figure 11 by using the energy level plot (upper left: partition curve) and the apparent loss factor plot (lower left): The analysis interval of T15 decay time (between -5 dB and -20 dB below starting energy level) corresponds to the time interval where the apparent loss factor has the plateau, leading to an average value of about 4%, again. For validation, the same value of about 4 % was found by analysing the experimental data of this reverberation situation for T15.

5.2. Impulse excitation of a thin partition wall

Relates to Figure 12. The impact is introduced approximately at the time point 240 ms. The excited thin partition wall contains all of the system's energy at this time and immediately starts to feed its neighbours (upper left plot). Since the partition is thin compared to its flanking walls, the coupling is bad and the flanking walls need a relatively long time to reach the same energy level as the partition. According to this, there is a long-lasting power flow (upper right plot) from the partition to the ceiling and other flanks. The power exchange between the partition and the room reverses approximately at 260 ms. Looking at the individual feedback terms (lower right plot), we find the rooms start affecting the partition's reverberation exactly at this point in time. The flanks hardly affect the apparent loss factor of the partition due to the weak coupling. Thus, we

find a time interval between the impact at 248 ms and the starting room influence at 260 ms, in which the reverberation process of the partition wall is not influenced by any neighbours. A T15 analysis yields a loss factor of about 4% which is indeed the total loss factor value. Reverberations analysis using longer time intervals such as T20 or T30 lead to definitely smaller loss factor values. Equivalent analysis of the experimental data validates these results.

5.3. Impulse excitation of a room

Relates to Figure 13. If the impact is introduced to the receiving room, then the system behaves in the classical way. The room has the smallest dissipation of all subsystems, so it serves as an energy buffer from the very first moment, feeding the walls which dissipate the energy (upper left plot). The power flows (upper right plot) only from the room to the surrounding walls. There is hardly any power reflow from the other subsystems (lower right plot) and the apparent loss factor is almost the total loss factor of the excited receiving room (lower left plot). A T15 analysis of the simulation yields a loss factor of about 0.2%, validated by the experimental data. This corresponds to a decay time of about 0.55 s at 2 kHz. On a full scale, this compares to about 5.5 s at 200 Hz which is typical for a medium or sparsely damped room. Indeed, the experiment confirms that the airborne decay of the excited room can also be measured by using the structure-borne sound on the adjacent walls.

5.4. Discussion

The main result of the TSEA analysis of the three situations is that no element acts independently, but all are part of a network spanning all building elements of the test facility. Energy is distributed over all elements and, in general, flows through any joint in any direction. When studying the reverberation of such a cross-linked system on any of its elements, the directly observed decay is strongly influenced by the network.

When the system is excited at any element, the reverberation process can generally be divided into two periods: a period of turbulent reverberation where energy is distributed over all subsystems, and a period of steady reverberation where the level differences between all subsystems remain constant and the system reverbs as a whole.

The deficiency of the simple (feedback-free) model demonstrates in several points: First, it is predicted that the power flows (upper right plots of Figures 11, 12 and 13) would decrease linearly (in level) over time and would only be directed out of the partition towards the neighbours and would never change direction. Against this, the experiment confirms the expanded model, as seen in Figures 8, 9 and 10.

Moreover, the simple model predicts the total loss factor of the excited subsystem to be determined in a standard T15 analysis. In opposite to this, the experiment validates the results of the expanded model, especially obviously for situation 5.1. Since, the expected total loss factor is about 12% whereas the measured one is only 4%, it is clear that power reflow can not be neglected here. Such an undervalued loss factor (about a factor of 3) would lead to undervaluing the damping influence on the sound reduction index of the example partition wall to about 5 dB. For situation 5.2, the agreement of the simple model with the experiment is purely coincidental. The detailed analysis using the expanded model shows that due to the decoupling of the flanks the requirements of the simple model are fulfilled for a short time period which is coincidentally sufficient for T15 analysis. But as can be seen in the lower right plot of figure 12, the influence of the rooms already affects the analysis time interval for T20 and T30 analysis leading to reduced loss factors.

This suggests that for loss factor analysis it would be better to define a certain pre-turbulent time period, where no network influence is expected, instead of a certain level decrease interval used by the T15 analysis procedure. Unfortunately, this unaffected time interval is different for each situation and, therefore, no unique rule seems to be applicable.

In the presented building acoustics examples, the energy reflow mainly affected the structure-borne reverberation (situations 5.1 and 5.2) and far less the airborne reverberation (situation 5.3). This is because of two reasons: Firstly, the two rooms did not couple directly with each other. Secondly, the rooms were weakly damped compared to the structure-borne elements and, therefore, served as an energy buffer in the system. Thus, reverberation measurements in the rooms of a standard wall test facility should be widely unaffected by network effects, in general. Nevertheless, network effects will emerge when airborne reverberation is studied in a room which is coupled to other rooms or other weakly damped elements (e.g. undamped lightweight elements). This is known in room acoustics as bent decay curves (see e.g. [21]). Unfortunately, modern building acoustics equipment usually only presents ready-to-read reverberation tables and hides the decay curves from the user, so network effects are often simply ignored.

6. Conclusions

Regarding the example of a standard two-room test facility for the measurement of the sound reduction index of separating building elements, it was shown that switching off the exciting sound signal will cause unsteady energy flows between all parts of the test facility including the air filled spaces and, of course, the specimen. Thus, the decay curve measured at any of the elements will represent a permanently changing combination of energy flows in and out of that element. The application of the simple and easy relation in (2) will result in damping values which are even lower than expected from material damping alone and which apparently change with time. Although unusual, these time-dependent "apparent damping factors" were kept here for a clearer distinction of the temporal changes of the energy flows (compared to the slope interpretation of decay curves) and because they approach

– under certain circumstances – real loss factors. Thus, they could be compared with otherwise known damping factors, or reveal information about which time segment of the reverberation curve would be best for interpretation. As an example, the very first moment of the decay curve seems to reflect approximately the total loss factor of an element, when having been excited directly, exclusively and by an impulse. But this time period lasts only a few milliseconds and is usually not even included in reverberation time evaluations. It is not clear yet how it can be used at all, lying in the settling times of the measurement equipment. In any case, the total loss factor values evaluated schematically from standard structural reverberation time measurements without regarding the energy reflow from the neighbourhood are not reliable but rather misleading in many cases. Intelligent interpretation of the decay can be nicely supported by a global transient SEA model.

The results of this paper also suggest that the effect of transient signals (like speech, traffic noise and most kinds of "living noise") on the sound reduction index of building elements should be identified.

Finally, the need still remains to determine and express the energy exchange between a building element and its surroundings to improve the comparability of measured results and to allow for a better prediction of insulation performance, when "moving" the building element from the laboratory into a building.

References

[1] L. Cremer, M. Heckl: Körperschall. Physikalische Grundlagen und technische Anwendungen. Springer, Berlin, Heidelberg, New York, 1996.

[2] C. Hopkins: Sound insulation: Theory into practice. Butterworth Heinemann, 2007. ISBN 978-0750665261.

[3] EN ISO 140-1:1997 + A1:2004: Acoustics. Measurement of sound insulation in buildings and of building elements. Part 1: Requirements for laboratory test facilities with suppressed flanking transmission. (ISO 140-1:1997 + AM 1:2004).

[4] EN 12354-1:2000: Building acoustics. Estimation of acoustic performance of buildings from the performance of products. Part 1: Airborne sound insulation between rooms.

[5] C. Kling: Investigations into damping in building acoustics by use of downscaled models. Dissertation RWTH Aachen. Aachener Beiträge zur Technischen Akustik, Band 7., Logos Verlag Berlin., 2008. http://darwin.bth.rwth-aachen.de/opus3/volltexte/2008/2514/.

[6] M. Schneider, F. Mack, H.-M. Fischer: Study of the influence of adjacent elements on the sound level decay of heavy building structures by means of transient SEA. NAG/DAGA, Rotterdam, 2009.

[7] C. Kling: Miniaturising a wall test facility. Building Acoustics **14** (2007) 243–266.

[8] C. Kling, M. Schmelzer: Measuring frequency-dependent material properties by use of N-parameter models. Acta Acustica united with Acustica **94** (2008) 568–579.

[9] R. J. M. Craik: Sound transmission through buildings: using statistical energy analysis. Gower Publishing Limited, 1996.

[10] R. H. Lyon, R. G. DeJong: Theory and application of statistical energy analysis. Second edition. Butterworth-Heinemann, Boston, 1995.

[11] W. Fasold, W. Kraak, W. Schirmer: Taschenbuch Akustik. 2. Auflage. VEB Technik, Berlin, 1984.

[12] R. H. Lyon, G. Maidanik: Power flow between linearly coupled oscillators. The Journal of the Acoustical Society of America **34** (1962) 623–639.

[13] R. H. Lyon, E. Eichler: Random vribration of connected structures. The Journal of the Acoustical Society of America **36** (1964) 1344–1354.

[14] J. Smith, P. W.: Response and radiation of structural modes excited by sound. The Journal of the Acoustical Society of America **34** (1962) 640–647.

[15] G. Maidanik: Response of ribbed panels to reverberant acoustic fields. The Journal of the Acoustical Society of America **34** (1962) 809–826.

[16] Y. E. Manning, K. Lee: Predicting mechanical shock transmission. Shock and vibration bulletin **37** (1968) 65–70.

[17] R. H. Lyon: Shock spectra for statistically modeled structures. Shock and vibration bulletin **40** (1969) 17–23.

[18] M. L. Lai, A. Soom: Prediction of transient vibration envelopes using statistical energy analysis techniques. Journal of Vibration and Acoustics **112** (1990) 127–137.

[19] M. J. Lai, A. Soom: Statistical energy analysis for the time-integrated transient response of vibrating systems. Transactions of the ASME **112** (1990) 206–213.

[20] L. Cremer, H. Müller: Principles and applications of room acoustics. Spon Press, 1982. ISBN 978-0853341130 and ISBN 978-0853341147.

[21] H. Kuttruff: Room acoustics. Fifth edition. Spon Press, 2009. ISBN 978-0415480215.

[22] ISO 140-3:1995 + AM 1:2004: Acoustics. measurement of sound insulation in buildings and of building elements. Part 3: Laboratory measurements of airborne sound insulation of building elements. Annex E.